An Multi-resources Integration Empowered Task Offloading in Internet of Vehicles: From the Perspective of Wireless Interference

Xiaowu Liu, *Member, IEEE*, Yun Wang, Kan Yu, *Member, IEEE*, Dianxia Chen, Dong Li, *Senior Member, IEEE*, Qixun Zhang, *Member, IEEE*, and Zhiyong Feng, *Senior Member, IEEE*

***Abstract*—The task offloading technology plays a vital role in the Internet of Vehicles (IoV), by satisfying the diversified demands of the vehicles, such as the energy consumption and processing latency of the computing task. Different from the previous works, on the one hand, they ignored the wireless interference of communications among vehicle-to-vehicle (V2V), as well as between vehicles and roadside units (RSU); on the other hand, the available resources of parked vehicles on the roadside and other moving vehicles on the road are also ignored. In this paper, first of all, we adopt a truncated Gaussian distribution for modeling the vehicle moving speed, instead of the simplistic average speed models in prior studies. Then, with the consideration of wireless interference and effective communication duration existing in V2V and RSUs, we establish an analytical framework of the task offloading, characterized by the energy consumption and processing delay, by integrating computing resources of parked/moving vehicles and RSUs. Furthermore, inspired by the method of multi-agent deterministic policy gradient (MADDPG), we address a joint optimization of the energy consumption and processing delay of the computing task, while ensuring the load balancing of the resources. Finally, the simulations demonstrate the effectiveness and correctness of the proposed MADDPG. In particular, compared with the current popular methods of the task offloading, the MADDPG shows the best performance, in terms of convergence speed, energy consumption and processing delay.**

***Index Terms*—Task offloading, wireless interference, energy consumption and processing delay, multi-agent deterministic policy gradient, convergence speed**

This work is supported by the Macao Young Scholars Program with Grants AM2023015, the National Natural Science Foundation of China with Grant 62301076, the Creative Research Groups of the National Natural Science Foundation of China with Grant 62321001, the Natural Science Foundation of Shandong Province with Grants ZR2021QF050 and ZR2021MF075, and the Science and Technology Development Fund, Macau SAR, under Grant 0029/2021/AGJ.

X. Liu is with School of Computer Science, Qufu Normal University, Rizhao, P.R. China. E-mail: liuxw@qfnu.edu.cn.

Y. Wang is with School of Computer Science, Qufu Normal University, Rizhao, P.R. China. E-mail:Yunwang321@126.com

K. Yu (the corresponding author) is with the School of Computer Science and Engineering, Macau University of Science and Technology, Taipa, Macau, 999078, P. R. China; the Key Laboratory of Universal Wireless Communications, Ministry of Education, Beijing University of Posts and Telecommunications, Beijing, 100876, P.R. China. E-mail: kanyu1108@126.com.

D. Chen (the corresponding author) is with the Education, Tianjin Ren'ai College, Tianjin, 301636, P.R.China. E-mail: chendianxia@tju.edu.cn.

D. Li is with the School of Computer Science and Engineering, Macau University of Science and Technology, Taipa, Macau, 999078, P. R. China. E-mail: dli@must.edu.mo.

Q. Zhang, and Z. Feng are with Key Laboratory of Universal Wireless Communications, Ministry of Education, Beijing University of Posts and Telecommunications, Beijing, 100876, P.R. China. E-mail: {zhangqixun, fengzy}@bupt.edu.cn.

I. Introduction

The Internet of Vehicles (IoV) is crucial for smart transportation, improving road safety, traffic efficiency, and environmental sustainability by facilitating information sharing among vehicles, roadside units (RSU), and traffic centers [1]. However, vehicles' limited computing resources hinder IoV's potential, prompting task offloading technologies that transfer computational tasks to RSUs, other vehicles, or the cloud, thereby enhancing computational capacity, reducing energy consumption, and supporting IoV operations [2]. Task offloading also optimizes network resource allocation, boosting data transmission efficiency and reliability, essential for seamless traffic unit coordination and advancing intelligent transportation systems.

The performance of the task offloading depends on the size and effective management of available resources provided by the system. Most of the current research efforts on resource expansions focused on the deployment of vehicle edge computing (VEC) and RSUs, under which the reduction of processing latency and energy efficiency of task offloading were considered. Subsequently, there are many works on the computational resources of task offloading, e.g., Q-Learning algorithms [3], multi-armed bandit (MAB) theoretical schemes [4] and the combination of deep learning and neural network technologies [5]. However, above popular methods ignored three key factors: processing delay, wireless interference in the processing of information exchange among various traffic units, and computing resources of individual vehicle. In detail,

1) The powerful computing resources of VEC and RSU usually are deployed in fixed servers or even the cloud, which provides a better QoS for vehicular task offloading, but the real-time requirements cannot be satisfied for different vehicles [6]. More important, when VEC and RSU satisfy the resources required for vehicular task offloading, and give the feedback on calculation results to the vehicle, the latter, caused by the mobility, may move off the communication range of VEC and RSU, resulting in a failure on the task offloading;
2) The information exchange and sharing among vehicle-to-vehicle (V2V) communications, and vehicle-to-infrastructure (V2I) communications involves wireless

communication interference, which further deteriorates the latency and reliability of the task offloading [7];

3) In fact, apart from powerful computation resources of VEC and RSU, the resources of pared vehicles on the roadside and moving vehicles on the road are also available, and they are more closer to the vehicles requesting for task offloading, which can provide a lower processing delay and higher reliability. Similarly, due to the mobility of vehicles, the communications among vehicles may be interrupted, resulting in a failure on the task offloading.

In view of the above three limitations on the current works for task offloading, in this paper, by integrating the computation resources of RSU, parked vehicles and moving vehicles, as well as the vehicular speed, cumulative communication interference, we established an analytical framework of task offloading in IoV. Furthermore, based on multi-agent deterministic policy gradient (MADDPG), we designed a task offloading to optimize the resource allocation, with the consideration of processing delay, energy consumption and wireless interference, and made a performance comparison with the traditional deep deterministic policy gradient (DDPG) in terms of the energy consumption and delay. The main contributions of the paper are summarized as follows.

1) We introduced a truncated Gaussian distribution for establishing a precise model of vehicle speeds and conducted a detailed analysis of communication interference among V2V and V2I. The analytical framework not only more accurately reflected the fluctuations in vehicle speeds and communication interference scenarios in real-world settings, but also provided precise estimations for delays, resource utilization, and effective communication time during the processing of task offloading. Consequently, this ensured that tasks were efficiently offloaded within the required latency limits.
2) By considering the computational resources of parked vehicles, moving vehicles and RSUs, it not only expanded the available resource scale and enhanced level of resources utilization, but also significantly reduced the processing delay of the computing task by offloading it to parked/moving vehicles and RSUs. Moreover, the introduction of the MADDPG algorithm for the joint optimization of delay and energy consumption effectively effectively achieved a balance between load balancing of the system and differentiated demand of the vehicles, in terms of energy consumption, processing delay and system cost.
3) Simulation results demonstrated the effectiveness and correctness of the proposed schemes. By making a performance comparison between the MADDPG and DDPG algorithms, the MADDPG algorithm showed a superior performance in key metrics, such as training efficiency, energy consumption, and delay optimization. Especially in scenarios involving complex multi-agent interference, the MADDPG algorithm exhibited a greater adaptability and efficiency, providing an effective solution for task offloading in complex scenarios. In addition, compared with other popular methods, such as LOCAL offloading [8], [9], V2V offloading [10], [11] and RSU offloading [12], [13], the MADDPG algorithm was still the best in terms of energy consumption and processing delay.

The remainder of the paper is organized as follows: Section II summarizes related works on task offloading and analyzes their advantages and limitations. In Section III, we present the network models, performance metrics and a joint optimization framework. Section IV presents the solutions for task offloading based on Reinforcement Learning (RL) and applies deep RL (DRL) to solve the optimization problem. Simulated results are reported and analyzed in Section V. Finally, conclusions and future works are discussed in Section VI.

II. Related Work

The resource allocation in IoV is a key technology when dealing with the task offloading. Computational resources for the task can be satisfied by RSUs or directly by vehicles, with the consideration of the energy consumption and processing delay, by utilizing edge computing, and V2I/V2V communications. In [14], Chen *et al.* proposed a task offloading scheme that relied solely on V2V communication by fully leveraging the idle resources of clustered vehicles. They formalized the task execution as a min-max problem between a task and multiple cooperative vehicles, and further solved it through the particle swarm optimization method. Extensive simulations showed that, through collaborative computing among vehicles, the model satisfied the latency requirements of latency-sensitive applications well. Furthermore, offloading tasks to RSUs was a popular method to solve the task offloading [15]. In [16], Zhu *et al.* discussed the issues of task offloading and computing resource allocation in the context of the IoV. In [17], Zhou *et al.* explored VEC networks based on RSUs and introduced a low-complexity distributed method to address the energy effectiveness of computing offloading decisions. In [18], Wang *et al.* designed a task offloading scheme that offloaded the task data to RSUs, and transformed the results to vehicles. But they overlooked the V2V offloading mode.

However, edge computing in V2I/V2V scenarios faces several challenges, and existing researches contributes to addressing task offloading and resource allocation issues under the VEC architecture. But they only focused on the V2I offloading mode. For vehicles outside the coverage range of RSUs, they suggested transmitting their task data to the RSU with the help of V2V communication relays. Considering the issue of task offloading empowered by V2V model, in [19], Feng *et al.* proposed a reverse offloading framework that fully utilized vehicular computational resources to alleviate the burden on VEC servers and further decreased the system latency. In [20], Xu *et al.* have delved into scenarios that leverage V2V communication relayed for vehicular task offloading in multi-edge computing environments. To fully explore the potential of increasingly powerful vehicles and their predictable mobility in enhancing the performance of dynamic networks, there are some challenges needing to be solved, such as incomplete offloading information, leading to worse system QoS and risks

of privacy leakage. Accordingly, in [21], Dai *et al.* developed a learning-based V2V offloading method, which was enhanced by the capabilities and trusted awareness of server vehicles. Moreover, in the proposed learning-based algorithm, both the QoS of server vehicles and secure V2V computing offloading were improved by using historical offloading selections to learn and predict the offloading performance of candidate server vehicles.

In fact, the V2I or V2V offloading schemes used separately cannot flexibly and accurately complete task offloading. To solve the problem, an increasing number of studies have considered the combination of V2I and V2V offloading model. To support the computationally intensive and latency-sensitive applications in the IoV, in [22], Hou *et al.* integrated computing resources of vehicles and these of RSUs together to provide low-latency computing services. Similarly, in [23], Huang *et al.* proposed a comprehensive VEC framework, designing a joint optimization for task type and vehicle speed-aware delay constraint model for both V2V and V2I offloading modes. Furthermore, in [24], Huang *et al.* proposed a MEC-based approach to address the issues of V2V/V2I offloading. By adopting MEC servers to collect information reported from vehicles, they then proposed a V2V/V2I offloading path selection method based on k-hop limited offloading time to find suitable V2V/V2I offloading paths. Simulation analyses showed that, under different settings of vehicle densities, the method they proposed outperformed traditional offloading schemes.

In short, above studies presented effective task offloading methods to address the significance of vehicles and RSUs' computational resources, and a fraction of them considered the effective communication duration, which is caused by the mobility of the vehicles, between vehicles and RSUs. In fact, on the one hand, with increasing vehicular computational capabilities, with the help of AI, the integration of V2V (moving on the road, especially parked on the roadside) and RSUs offloading modes can alleviate the burdens of individual vehicle and RSU, which further enhances the performance of energy consumption, processing delay and resource loading balancing. On the other hand, more important, wireless interference caused by communications among vehicles or between vehicles and RSUs exists, and affects the success probability of task offloading, energy consumption and processing delay, which are ignored by all above works.

III. Network Model and Preliminaries

As shown in Fig. 1, a vehicular edge computing model is considered, consisting of a base station (BS), H RSUs and K moving vehicles, and M parked vehicles. Constrained by limited power resources, the coverage area of an RSU is defined as a circular region with the radius of r, and the vertical distance from the road is $d_{rsu,ver}$. The location of the i-th RSU is denoted by $\mathbf{t}_{rsu_i} = [x_{rsu_i}, y_{rsu_i}, z_{rsu_i}]^T$ ($1 \leq i \leq H$). The moving vehicles in both directions and parking vehicles can be covered by an RSU at least. The location of the j-th moving/parking vehicle is denoted by $\mathbf{t}_{ve_j} = [x_{ve_j}, y_{ve_j}]^T$, and the speed and direction of k-th

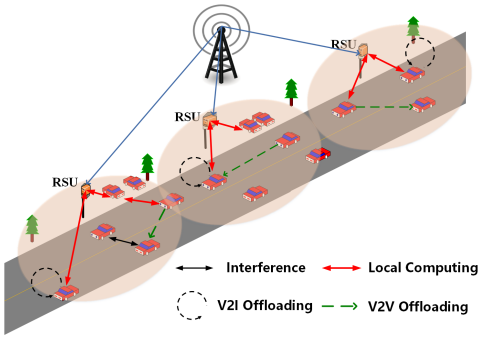

Fig. 1. Simulation results for the network.

moving vehicle are denoted by v_k and x, respectively, the moving direction can be represented as the sign of v_k.

Under the above model, H RSUs, M parked vehicles and a fraction of moving vehicles with no demands of task offloading can integrate and utilize their resources to support the task offloading initiated by moving vehicles. An RSU, along with parked vehicles within its coverage area, only provides computation resource to the moving vehicles within its coverage area, and the interference between different coverage area of RSUs can be ignored securely since the interference caused by task offloading in current area is more severe. In addition, RSUs can monitor the status of the computation resources supported by the vehicles, and decide whether to process the task data by using integrated resources or offload the data to the BS, based on the sate of current resource utilization, energy consumption and different requirements of vehicles.

A. The Speed Model of Moving Vehicles

Due to the vehicular mobility and limited coverage area of RSUs, for a given moving vehicle with requesting task offloading, there is a potential disconnection between it and RSUs or other vehicles with supporting computation resources, resulting in failing to do the tasking offloading. To deal with this problem, a truncated Gaussian distribution model is introduced to the study of vehicle traffic theory, since the speed follows the Gaussian distribution law. On the one hand, it can accurately reflect the driving speed of vehicles while ensuring the feasibility and timeless of the speed. On the other hand, the model can comprehensively describe the dynamic behaviors of vehicles, namely the duration time that moving vehicles can keep effective communications with an RSU within its coverage area, or that among vehicles.

B. The Speed Description of Moving Vehicles

Traditionally, simplified mean speed model usually is adopted to simulate the vehicular velocity, which uses constant speeds or considers only a few distinct speed levels to describe the vehicle motion. However, the model ignores the speed variability and dynamic traffic conditions, resulting in a failure to accurately characterize fluctuations of vehicular speed under real conditions, such as traffic flow, road conditions and traffic signals. We assume that each vehicle enters the segment at a random speed. Accordingly, it is assigned a speed v

TABLE I
SYMBOLS AND MEANINGS

symbols	meanings	Symbols	meanings
H	number of RSUs	K	number of moving vehicles
M	number of parked vehicles	r	coverage radius of RSU projections
$d_{rsu,ver}$	vertical distance from RSUs to road	$\mathbf{t}_{rsu_i}$	location of i-th RSU
t_{ve_j}	location of j-th moving/parking vehicle	v_k	speed of k-th moving vehicle
F^I	maximum CPU cycle frequencies of vehicle	F^R	maximum CPU cycle frequencies of RSU
$f_v(v)$	PDF of Gaussian distribution	p_{ve_k}	transmission power of k-th vehicle
$\mathrm{erf(x)}$	Gaussian error function	R_{ve_k,ve_i}	transmission rate between k-th and i-th vehicles
$v_k(t)$	equivalent speed of k-th vehicle in time slot t	R_{ve_k,r_i}	transmission rate between k-th vehicle and i-th RSU
h_{ve_k,r_i}	channel coefficient between k-th vehicle and i-th RSU	d_{ve_k,r_i}	distance between k-th vehicle and i-th RSU
$\sigma^2_{r_i}$	AGWN power at i-th RSU	δ_{ve_j,r_i}	j-th vehicle is associated with i-th RSU or not
$\sigma^2_{ve_i}$	AWGN power at i-th vehicle	$Z_{ve_k}(t)$	processing density
δ_{ve_j,ve_k}	j-th and k-th vehicles are associated or not	Ψ_{ve_k}	set of candidate offloading decisions
$\widetilde{f_v}(v)$	speed under a truncated Gaussian distribution	$H_{ve_k}(t)$	The size of the task
τ_{ve_k}	task priority	$T_{\max}(t)$	affordable maximum latency of the task
$D^{ve_k}_{ve_k}(t)$	delay offloading to vehicle	$f^{ve_k}_{r_i}(t)$	CPU cycle allocated to k-th vehicle by i-th RSU
$D^{r_i}_{ve_k}(t)$	delay Offloading to RSU	p_{ve_k}	transmission power of the vehicle
P_{ve}	calculated power of the vehicle	$E^{ve_k}_{ve_k}(t)$	energy consumption offloading to other vehicles
$E^{r_i}_{ve_k}(t)$	energy consumption offloading to RSU	$S(t)$	state space of vehicle at time slot t
$A(t)$	action of vehicle at time slot t	$R(s(t),a(t))$	calculation of cumulative rewards
γ	discount factor for balancing rewards	Q_{ve}	state-action value function of the target network

determined by a Gaussian distribution. To further make the study more realistic and avoid the case of negative velocity, the speed v is constrained by a truncated Gaussian distribution [25] [26]. That is, the probability density function (PDF) of a given speed v under a truncated Gaussian distribution can be represented as

$$\widetilde{f}_v(v) = \frac{f_v(v)}{\int_{v_{\min}}^{v_{\max}} f_v(s)\,ds} = \frac{2f_v(v)}{\mathrm{erf}(\frac{\mathrm{v_{max}}-\mu}{\sigma\sqrt{2}}) - \mathrm{erf}(\frac{\mathrm{v_{min}}-\mu}{\sigma\sqrt{2}})} \quad (1)$$

where μ and σ denote the mean velocity and standard deviation of the truncated Gaussian distribution, respectively, $f_v(v) = (1/\sigma\sqrt{2\pi})\exp(-((v-\mu)^2/2\sigma^2))$ is the PDF of the Gaussian distribution, $\mathrm{erf(x)} = (2/\sqrt{\pi})\int_0^{\mathrm{x}} \mathrm{e}^{-\mathrm{s}^2}\mathrm{ds}$ is the Gaussian error function, and $v_{\min} = \mu - 3\sigma$ and $v_{\max} = \mu + 3\sigma$ are the minimum and maximum vehicular speeds, respectively.

According to the PDF in Eq. (2), the equivalent speed of the k-th vehicle in time slot t can be described as

$$v_k(t) = \frac{1}{\int_{v_{\min}}^{v_{\max}} \frac{\widetilde{f_v}(v)}{v}\,dv} = \frac{\mathrm{erf}(\frac{\mathrm{v_{max}}-\sigma}{\sigma\sqrt{2}}) - \mathrm{erf}(\frac{\mathrm{v_{min}}-\sigma}{\sigma\sqrt{2}})}{\frac{2}{\sigma\sqrt{2\pi}}\int_{v_{\min}}^{v_{\max}} \frac{\exp(-\frac{(v-\sigma)^2}{2\sigma^2})}{v} dv} \quad (2)$$

1) The Duration Description between vehicles and RSUs: Constrained by the limited coverage area of RSUs, vehicular mobility and direction of vehicular speed, the communication distance between vehicles and RSUs is a random variable, and becomes a crucial parameter, since it affects the result of task offloading. In other words, when the duration time of keeping effective communications is less than that of task offloading, the RSU cannot return the result of task offloading to the vehicle successfully. Based on the location model and speed model in Eq. (2), the distance between the k-th vehicle and the the i-th RSU, denoted by d_{ve_k,r_i}, can be given as

$$d_{ve_k,r_i} = \begin{cases} x_{rsu,i} + \sqrt{r^2 - d^2_{rsu,ver}} - x_{veh,k}, v_k(t) > 0 \\ x_{veh,k} - (x_{rsu,i} - \sqrt{r^2 - d^2_{rsu,ver}}), v_k(t) < 0 \end{cases} \quad (3)$$

where $\sqrt{r^2 - d^2_{rsu,ver}}$ denotes the half of the coverage length of the RSU on the road, and positive and negative signs of v_k describe the moving direction of the k-th vehicle ve_k.

Therefore, the duration that the k-th vehicle ve_k and the i-th RSU r_i keep success communications in time slot t before moving out of the latter's coverage area can be calculated by $t^{\mathrm{hold}}_{ve_k,r_i} = \frac{d_{ve_k,r_i}}{|v_k(t)|}$. That is, the duration of keeping effective communications is the range of $[t, t^{\mathrm{hold}}_{ve_k,r_i}]$.

The duration among vehicles: Let L be a constant value and denote the maximum distance that any two vehicles can keep effective communication in V2V. Therefore, the duration of V2V communication between the k-th vehicle ve_k and the j-th vehicle ve_j (moving vehicle or parked vehicle), denoted by $t^{\mathrm{hold}}_{ve_k,ve_j}$, can be calculated as

$$t^{\mathrm{hold}}_{ve_k,ve_j} = \begin{cases} \left|\frac{L - |x_{ve_k}(t) - x_{ve_j}(t)|}{v_{ve_j}(t) - v_{ve_k}(t)}\right|, L - |x_{ve_k}(t) - x_{ve_j}(t)| \geq 0, \\ \frac{|x_{ve_k}(t) - x_{ve_j}(t)|}{v_{ve_k}(t) - v_{ve_j}(t)} \geq 0 \\ 0, L - |x_{ve_k}(t) - x_{ve_j}(t)| < 0 \\ \left|\frac{2L - |x_{ve_k}(t) - x_{ve_j}(t)|}{v_{ve_j}(t) - v_{ve_k}(t)}\right|, L - |x_{ve_k}(t) - x_{ve_j}(t)| \geq 0, \\ \frac{|x_{ve_{ve_k}}(t) - x_{ve_j}(t)|}{v_{ve_k}(t) - v_{ve_j}(t)} < 0 \end{cases} \quad (4)$$

where the segmented function is designed to calculate the effective duration of V2V communication when two vehicles are within the communication range. The first segment of the function denotes the time between vehicles ve_k and ve_j, moving in the same direction. The second segment indicates that

effective duration of V2V communication between vehicles ve_k and ve_j becomes zero when they are not within the communication range. The third segment represents the effective duration for vehicles ve_k and ve_j when they are moving in opposite directions but still within the communication range.

C. The Delay Analysis of Task Offloading

The delay of task offloading between moving vehicles and RSUs or vehicles with no demands of task offloading is highly related to their transmission rates, while the channel condition, communication distance and transmission power, and particularly the cumulative interference caused by non-intended communications are key factors in affecting the transmission rate. Therefore, it is of great significance to accurately establish the model of transmission rate and delay to optimize the resource management of IoV with the consideration of the accumulated wireless interference, which can provide a more efficient task offloading strategy for IoV.

1) Transmission Rate between Vehicles and RSUs with Cumulative Interference: Combining with the conclusions in [27] [28], the transmission rate between the k-th moving vehicle ve_k with requiring a task offloading and the i-th RSU r_i covering the k-th moving vehicle, denoted by R_{ve_k,r_i}, can be represented as

$$R_{ve_k,r_i} = W\log_2(1+\frac{p_{ve_k}h_{ve_k,r_i}d_{ve_k,r_i}^{-\alpha}}{\sigma^2+\sum\limits_{j=1,j\neq k}^{K}\frac{p_{ve_j}h_{ve_j,r_i}}{d_{ve_j,r_i}^{\alpha}}\cdot\delta_{ve_j,r_i}}) \quad (5)$$

where W is the transmission bandwidth, p_{ve_k} is the transmission power of the k-th vehicle, h_{ve_k,r_i} and d_{ve_k,r_i} are the Rayleigh fading channel coefficient and the distance between the k-th vehicle and the i-th RSU. In particular, h_{ve_k,r_i} follows an exponential distribution with unit mean. α is the path-loss exponent, and $\sigma_{r_i}^2$ is the additive Gaussian white noise (AGWN) power. Moreover, the indicator function $\delta_{ve_j,r_i} \in \{0,1\}$ represents whether the j-th vehicle is associated with the i-th RSU r_i or not. Specifically, $\delta_{ve_j,r_i}=1$, if the j-th vehicle requests a task offloading and is within the coverage of the i-th RSU r_i; otherwise, $\delta_{ve_j,r_i}=0$, namely the j-th vehicle does not be with no need for a task offloading, or is not within the coverage range of the i-th RSU.

2) Transmission Rate among Vehicles with Cumulative Interference: The transmission rate between the k-th moving vehicle the ve_k with requiring a task offloading and the i-th moving/parked vehicle ve_i supporting computing resources to the former, denoted by R_{ve_k,ve_i}, can be represented as

$$R_{ve_k,ve_i} = W\log_2(1+\frac{p_{ve_k}h_{ve_k,ve_i}d_{ve_k,ve_i}^{-\alpha}}{\sigma^2+\sum\limits_{j=1,j\neq k,j\neq i}^{K}\frac{p_{ve_j}h_{ve_j,ve_i}}{d_{ve_j,ve_i}^{\alpha}}\cdot\delta_{ve_j,ve_k}}) \quad (6)$$

where $\sigma_{ve_i}^2$ denotes the AWGN power at the i-th vehicle, and the indicator function $\delta_{ve_j,ve_k} \in \{0,1\}$ denotes whether the j-th vehicle and the k-th vehicle are both within the coverage area of the same RSU. Specifically, $\delta_{ve_j,ve_k}=1$, if the j-th vehicle sends a task offloading to the RSU, which has been assigned its resources to the k-th vehicle for achieving the task data processing; otherwise, $\delta_{ve_j,ve_k}=0$.

3) Delay analysis: Considering a binary task offloading where the moving vehicle with the demand of task offloading chooses to process the computing task locally or offload the task to a RSU or an unoccupied vehicle (parked vehicle and moving vehicle with no demands of task offloading) within their effective communications. Due to the mobility characteristics of vehicles, for a given the k-th vehicle with the demand of task offloading, available computing resources are dynamic. Let $\Psi_k(t)$ be the set of candidate offloading decisions for the k-th vehicle ve_k at time slot t, consisting of RSUs, moving vehicles and parked vehicles. Accordingly,

$$\begin{aligned}\Psi_{ve_k}(t) = &\{\Psi_{ve_k}^{ve_1},...,\Psi_{ve_k}^{ve_{k-1}},\Psi_{ve_k}^{ve_{k+1}}...,\Psi_{ve_k}^{ve_K}\}\\ &\cup\{\Psi_{ve_k}^{r_1},...,\Psi_{ve_k}^{r_H}\}\cup\{\Psi_{ve_k}^{ve_1},...\Psi_{ve_k}^{ve_M}\}\end{aligned}$$

where $\Psi_{ve_k}^{m}$ for any m is a binary random variable and denotes a offloading decision, namely the k-th vehicle offloads its task data to the m-th unoccupied resource. In detail, $\Psi_{ve_k}^{m}=1$ the task data of the k-th vehicle is offloaded to m-th unoccupied resource node; otherwise, $\Psi_{ve_k}^{m}=0$. In addition, $\Psi_{ve}(t)$ denotes the set of candidate offloading decisions for all vehicles. Furthermore, we introduce three kinds of task offloading models and corresponding delay analyses. Specially, we assume that the RSU and the base station are connected by high transmission lines, so that the data transmission delay between the RSU and the base station is negligible.

The time frame when executing task offloading of any moving vehicle is discredited into multiple decision epoches. At the begin of decision epoch t, a task, featured by periodic, computation-intensive and indivisible, needs to be executed in the k-th moving vehicle, and can be modeled as as $S_{ve_k} \triangleq \{H_{ve_k}(t), Z_{ve_k}(t), T_{\max}(t), \tau_{ve_k}\}$, where $H_{ve_k}(t)$ denotes the size of the original task data, $Z_{ve_k}(t)$ (in CPU cycles/bit) denotes the processing density (i.e., the number of CPU cycles needed per unit of data), $T_{\max}(t)$ (in ms) denotes the affordable maximum latency requirement of the task, $\tau_{ve_k} \in \{0,1\}$ signifies the task priority. In other words, $\tau_{ve_k}=1$ indicates that high-priority tasks require immediate execution, while $\tau_{ve_k}=0$ suggests that low-priority tasks can be executed at any time within the affordable maximum latency constraints.

1) Local Offloading Model: For the case of $\tau_{ve_k}=1$ of the k-th vehicle with demands of task offloading in time slot t, it first resorts to local offloading (i.e., offloading the task data to its computing resource) if the resource is enough available, and corresponding delay is minimized. Otherwise, it will execute the following second and third task offloading schemes. Let F^I be the maximum CPU cycle frequencies of the vehicle. Thus, the delay of a task offloading in local offloading model in time slot t, denoted by $D_{ve_k}^{ve_k}(t)$, can be represented as $D_{ve_k}^{ve_k}(t)=\frac{H_{ve_k}(t)Z_{ve_k}(t)}{F^I}$, where F^I denotes the computation capacity, i.e., maximal CPU-cycle frequency of the vehicle; otherwise, the vehicle fails to request a task offloading, and will execute other task offloading schemes.

2) V2V Offloading Model: Once the computation resource of the k-th moving vehicle, resulting in a failure on the local offloading, considering the latency requirement constraint of the k-th vehicle, it offloads the task data to a moving vehicle or a parked vehicle at the roadside within the effective communication range. Based on the maximum CPU-cycle frequency of the vehicle F^I and transmission rate in Eq. (6), the delay of executing a task offloading to the j-th vehicle can be calculated as $D_{ve_k}^{ve_j}(t) = \frac{H_k(t)Z_k(t)}{F^I} + \frac{H_k(t)}{R_{ve_k,ve_j}}$, and $D_k^k(t) \leq t_{ve_k,ve_j}^{\text{hold}}$ for the constraint of the latency.

3) RSU Offloading Model: When the local offloading model and vehicle offloading model fail, which means that there is no available vehicles with enough computation resources for supporting the task offloading, the task data will be offloaded to RSUs. To process multiple computing task simultaneously, the dynamic frequency and voltage scaling technique are adopted in the RSUs, which can dynamically allocate available resources of the CPU frequency [29]. Let $\xi_{r_i}(t)$ be the whole computation resource requirements of multiple tasks served by the i-th RSU r_i, and $f_{r_i}^{ve_k}(t) = (H_{ve_k}(t)Z_{ve_k}(t)/\xi_{r_i}(t))^* F^R$ be the CPU-cycle frequency allocated to the k-th vehicle ve_k by the i-th RSU r_i, where F^R denotes the maximum CPU-cycle frequency of the RSU. Accordingly, the computation delay can be represented as $D_{ve_k}^{r_i}(t) = H_{ve_k}(t)Z_{ve_k}(t)/f_{r_i}^{ve_k}(t)$. Furthermore, the delay of offloading the task to the RSU can be calculated as $D_{ve_k}^{r_i}(t) = D_{ve_k}^{r_i}(t) + \frac{H_{ve_k}(t)}{R_{ve_k,r_i}}$, and $D_{ve_k}^{r_i}(t) \leq t_{ve_k,r_i}^{\text{hold}}$.

In summary, regardless of whether offloading occurs to parked vehicles, moving vehicles, or RSUs, the execution delay can be represented as

$$D_{ve_k}^{\text{sum}}(t) = \Psi_{ve_k}^{ve_k} D_{ve_k}^{ve_k}(t) + \Psi_{ve_k}^{ve_j} D_{ve_k}^{ve_j}(t) + \Psi_{ve_k}^{r_i} D_{ve_k}^{r_i}(t) \quad (7)$$

D. Energy Consumption Model

The energy consumption is a key metric in the task offloading of a IoV, including the transmission power, calculation power of the task data and energy consumption power coefficients of each unit CPU cycle. A effective energy consumption model involves local calculation energy consumption, and the consumption for offloading the task data to moving/parked vehicles and RSUs, which can provide a an analytical framework for evaluating the energy efficiency of different task offloading strategies. Based on the closed-form expression of total energy consumption, the performance difference of different task offloading schemes can be quantified more intuitively.

1) The energy consumption of the local offloading model: Let P_{ve} be the calculating power of the vehicle. When the resources of the vehicle requesting a task offloading can meet the performance constraints of the task, the corresponding energy consumption can be given as $E_{ve_k}^{ve_k}(t) = P_{ve}H_{ve_k}(t)Z_{ve_k}(t)/F^I$.

2) The energy consumption of the vehicle offloading model: Combined with the transmission rate in Eq. (6) and maximum CPU-cycle frequency of the vehicle, the energy consumption of offloading the task data to one of vehicles with enough computation resources, denoted by the j-th vehicle, can be calculated as $E_{ve_j}^{ve_k}(t) = \frac{P_{ve}H_{ve_k}(t)Z_{ve_k}(t)}{F^I} + p_{ve_k}\frac{H_{ve_k}(t)}{R_{ve_k,ve_i}}$.

3) The energy consumption of the RSU offloading model: Let P_r denote the calculating power of the RSU. Similarly, the energy consumption of offloading the task data to the RSU with enough computation resources can be represented as $E_{ve_k}^{r_i}(t) = \frac{P_{r_i}H_{ve_k}(t)Z_{ve_k}(t)}{f_{ve_k}^r(t)} + p_{ve_k}\frac{H_{ve_k}(t)}{R_{ve_k,r_i}}$.

To sum up, the total energy consumption of the vehicle with the demands of task offloading can be given by

$$E_{ve_k}^{\text{sum}}(t) = \Psi_{ve_k}^{ve_k} E_{ve_k}^{ve_k}(t) + \Psi_{ve_k}^{ve_j} E_{ve_k}^{ve_j}(t) + \Psi_{ve_k}^{r_i} E_{ve_k}^{r_i}(t) \quad (8)$$

E. Problem Formulation

The energy consumption and processing delay of task offloading are two key factors in measuring the performance of an IoV. These factors are constrained by the interference generated by non-intended vehicles, the affordable maximum latency of the task, offloading decisions, the duration of effective communications, and the calculating powers of vehicles or RSUs. Let α_{ve_k} and β_{ve_k} denote the weight factor for satisfying the constraints of delay and energy consumption for the k-th vehicle. Given multiple task offloadings requesting by moving vehicles, to balance the processing delay and energy consumption of the vehicle, we establish an optimization framework to minimize the total the energy consumption and processing delay of all vehicles simultaneously as follows.

$$\text{Object:} \quad \min_{\Psi_{ve}(t)} \sum_{k=1}^{K} (\alpha_{ve_k} D_{ve_k}^{\text{sum}}(t) + \beta_{ve_k} E_{ve_k}^{\text{sum}}(t)) \quad (9a)$$

$$\text{s.t.} \quad \alpha_{ve_k} + \beta_{ve_k} = 1, \forall \alpha_{ve_k} \in [0,1], \beta_{ve_k} \in [0,1] \quad (9b)$$

$$\Psi_{ve_k}^m(t) \in \{0,1\}, \forall k, m \quad (9c)$$

$$\sum_{\Psi_{ve_k}^m \in \Psi_{ve_k}(t)} \Psi_{ve_k}^m \leq 1, \ \forall m, k \quad (9d)$$

$$D_{ve_k}^{\text{sum}}(t) \leq T_{\max}(t), \ \forall k \quad (9e)$$

$$P_{ve} < P_r \quad (9f)$$

$$\Psi_{ve_k}^{ve_j}(t) D_{ve_k}^{ve_j}(t) \leq t_{ve_k,ve_j}^{\text{hold}}, \forall k, j \quad (9g)$$

$$\Psi_{ve_k}^{r_i}(t) D_{ve_k}^{r_i}(t) \leq t_{ve_k,r_i}^{\text{hold}}, \forall k, j \quad (9h)$$

where Eq. (9c) and Eq. (9d) are offloading decision constraints, Eq. (9e) is the offloading decision constraint, Eq. (9f) is the calculating power constraint, Eq. (9g) and Eq. (9h) are constraints on effective communication duration.

IV. Task Offloading Algorithms based on Reinforcement Learning (RL)

A. Task Offloading Algorithm Based on Multi-Agent RL

The performance of task offloading is affected by complex interference and vehicular mobility, multiple vehicles behave cooperatively and competitively, which is a typical NP-hard problem [30]. To effectively address the issue, in this section, we adopt a deep RL approach to model the process of

task offloading and resource allocation decision, and further accurately capture the dynamic characteristics of the IoV.

When the external parameters varies with different time slots, and the optimal variables are adjusted accordingly, then above optimization problem can be transformed into a MDP [31], which can be represented as a tuple of $\{S, A, P, R\}$, where $S = \{s(1),,, s(t), ..., s(T)\}$ denotes the state space, i.e., the set of parameters varying over time slot t, A denotes the action space, i.e., the set of optimization variables changing over time slot t, we consider that a model-free multi-agent reinforcement learning task that ignores the state transition function $P = \Pr[s(t+1)|s(t), a(t)]$, R is the reward function, namely a value space of the optimization problem related to a decision action $a(t)$ and state $s(t)$, denoted by $r(s(t), a(t))$. To sum up, a MDP can be executed as follows. Based on the current state $s(t)$ at time slot t [32], it selects an action $a(t)$ from the action space as a final decision. Parameter $\gamma \in [0, 1]$ is the discount factor describing the balance between current and future rewards. A tuple of $\{S, A, P, R\}$ is further described as follows.

1)State Space: Each vehicle is regarded as an agent, and its local observation value is $s_{ve_k}(t) \in S_{ve}(t)$, where S_t^{ve} is the local observation value of all vehicles at time slot t, including five parts: coordinates, data size, demand of computation resource, delay, and delay gain. Accordingly, the local observation results of all vehicles at time slot t can be represented as

$$S_{ve}(t) = [\theta_{ve}(t), H_{ve}(t), Z_{ve}(t), T_{\max}, \tau_{ve}(t)] \tag{10}$$

2) Action Space: The action of agent ve_k at time slot t is the task offloading decision, denoted by $a_{ve_k}(t) \in A_{ve}(t)$, where is the action of all vehicles at time slot t, which can be represented as

$$A_{ve}(t) = [\Psi_{ve_1}(t), ..., \Psi_{ve_k}(t), ..., \Psi_{ve_K}(t)] \tag{11}$$

3) Reward: In collaborative multi-agent deep reinforcement learning model, when executing a task cooperation, all agents cooperate to make unloading decisions, and all agents share team rewards to maximize the shared global system-level rewards. From Eq. (9a), it can be seen that the objective function is to minimize the time delay and energy consumption. The author of [33] have shown that the best unloading policy can be found by maximizing a negative reward. Therefore, the reward function of the MDP can be defined as

$$r(s(t), a(t)) = -\sum_{k=1}^{K} (\alpha_{ve_k} D_{ve_k}^{\text{sum}}(t) + \beta_{ve_k} E_{ve_k}^{\text{sum}}(t)) \tag{12}$$

Accordingly, applying this reward function to calculate cumulative rewards, for the k-th agent ve_k, its cumulative reward, denoted by $R(s(t), a(t))$, can be written as

$$R(s(t), a(t)) = \sum_{t=0}^{t=T} \gamma(t) \cdot r(s(t), a(t)) \tag{13}$$

B. Multi-Agent Deep RL (DRL) Algorithms

To deal with the "curse of dimension" problem [34] caused by DQN when facing the state space of multiple agents successfully, we approximate the value function of each agent's policy and environment interaction by integrating the neural network.Similar to the DQN algorithm, the empirical replaying mechanism is also applied to further improve the learning efficiency of neural networks, which is batched by using small batch sampling and storing multi-step samples. This approach aims to update network parameters at different CPU frequencies by using the target network. Here, "different CPU frequencies" refers to varying the speed at which the algorithm updates its knowledge base, allowing for a balance between rapid learning from new data and maintaining stability from past learning. Furthermore, MADDPG algorithm also adopts the advantages of policy gradient scheme and DQN, including two kinds of neural networks: policy-based actor (Actor) networks and value-based reviewer (Critic) networks. In detail, the Actor network performs the actions based on the corresponding collected environmental states, while the Critic network evaluates the value of selected actions based on the strategy. Here, the strategy refers to the learned policy that guides how tasks are offloaded in the vehicular network environment, aiming to optimize for factors such as energy consumption and task completion time. The policy evolves through interaction with the environment, adjusting based on the feedback evaluated by the Critic network to find the most efficient offloading decisions given the current state and potential future states. Let $R(s(t), a(t))$ be the immediate reward of the vehicle at the time slot t. The state-action value function of the MADDPG algorithm can be expressed as

$$Q_{ve}(\mathbf{S}_t, \mathbf{A}_t) = E\left[R(s(t), a(t)) + \gamma Q_{ve}(\mathbf{S}(t+1), \mathbf{A}(t+1))\right] \tag{14}$$

where E is an expectation function for all possible subsequent states $\mathbf{S}(t+1)$ and the corresponding actions $\mathbf{A}(t+1)$, as well as the potential rewards $R(s(t), a(t)$. The expected operation enables MADDPG to evaluate the overall utility of the current actions within a complex multi-agent environment. Here,$\mathbf{S}(t)$ and $\mathbf{A}(t)$ represent the set of all agents' states and actions, respectively, at time slot t, and $Q_{ve}(\mathbf{S}(t+1), \mathbf{A}(t+1))$ denotes the state-action value function for the next time slot $t+1$.

The MADDPG algorithm aims to determine a set of optimal strategies for all agents, denoted by π_{ve}. Each optimal strategy of any agent determines the actions an agent takes based on its observation of the environment. Each strategy in set of π_{ve} guides agents on how to interact with the environment to maximize their cumulative rewards. Through learning, agents adapt their strategies to make better decisions over time, aiming to converge to the optimal strategy that maximizes their individual and collective rewards. Therewith, MADDPG adopts a dual network structure of the Actor-Critic network, consisting of an evaluation network (Actor parameter is θ_{ve}^{μ}, and Critic parameter is θ_{ve}^{Q}), and a target network (Actor parameter is $\theta_{ve}^{\mu'}$, and Critic parameter is $\theta_{ve}^{Q'}$). Specifically, the parameters of each agent's evaluation network, the Actor network, and the Critic network are updated in real time with

$$L(\theta_{ve}^{Q}) = E\left[\left(R(s(t),a(t)) + \gamma Q'_{ve}(\mathbf{S}(t+1),\mathbf{A}(t+1)|\theta_{ve}^{Q'}) - Q_{ve}(\mathbf{S}(t),\mathbf{A}(t)|\theta_{ve}^{Q})\right)^2\right] \quad (15)$$

where $Q'_{ve}(\cdot)$ represents the state-action value function of the target network.

the following steps: First, a small batch of data samples are randomly sampled from the experience pool, which are then input into each agent's network. During training, the Actor network generates actions according to the current strategy, while the Critic network evaluates the value of these actions. Critic the parameters of the network are updated by minimizing the gap between the actual and predicted returns, which is usually done by calculating the loss function and applying a gradient descent method. In addition, the parameters of the Critic's evaluation network can be updated by minimizing the following loss function in Eq. (15).

The parameter of θ_{ve}^{Q} in Eq. (15) can be adjusted with the gradient of the loss function, when the function of $L(\theta_{ve}^{Q})$ is continuously differentiable. Then the Actor network makes action decisions for each observation, namely each agent aims to maximize cumulative returns. the parameters of the Actor's evaluation network can be updated by maximizing the policy objective function as follows.

$$J(\theta_{ve}^{\mu}) = E\left[Q_{ve}(\mathbf{S}(t),\mathbf{A}(t)|\mathbf{A}(t)=\mu(\mathbf{S}(t)|\theta_{ve_k}^{\mu})\right] \quad (16)$$

where $\mu_{ve}(\cdot)$ is a deterministic policy function of the Actor evaluation network, which makes a mapping relationship between the states to the actions, namely a set of strategies π_{ve}. If the action space is continuous, then $J(\theta_{ve}^{\mu})$ is continuously differentiable, under which the direction of gradient descent, denoted by $\bigtriangledown_{\theta_{ve}^{\mu}} J(\theta_{ve}^{\mu})$, can be adjusted by updating the parameter of θ_{ve}^{μ}. In addition, as the parameters θ_{ve}^{μ} and θ_{ve}^{Q} of the evaluation network are continuously updated, the parameters $\theta_{ve}^{\mu'}$ and $\theta_{ve}^{Q'}$ of the target network can be updated as follows, by using a soft update method, which applies a weighted averaging when updating the parameters of the target network, so that the parameters of the target network are relatively smoothly close to the parameters of the evaluated network during the update process. Specifically, given a parameter update rate ϖ, the parameters of the target network $\theta_{ve}^{\mu'}$ and $\theta_{ve}^{Q'}$ can be updated as follows.

$$\theta_{ve}^{\mu'} = \varpi\theta_{ve}^{\mu} + (1-\varpi)\theta_{ve}^{\mu'} \quad (17)$$

$$\theta_{ve}^{Q'} = \varpi\theta_{ve}^{Q} + (1-\varpi)\theta_{ve}^{Q'} \quad (18)$$

where $\varpi \ll 1$ is a small positive constant, which is used to control the updating speed of the target network's parameters and ensure the stability of the learning process. This approach facilitates collaboration among agents and enables them to move together towards the optimal strategy. Meanwhile, to simplify the training process, each agent network is allowed to share the weights, which helps to reduce the complexity of the required processing.

As described above, corresponding frameworks of DDPG and MADDPG are presented as follows.

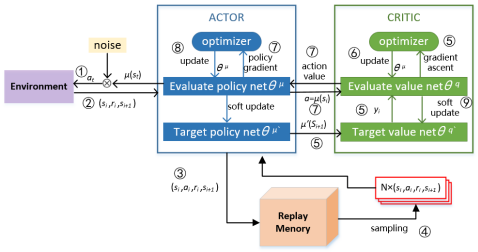

Fig. 2. The framework of DDPG.

DDPG framework: To better highlight the performance of MADDPG and make a comparison with MADDPG, we first describe the framework DDPG for the problem of task offloading of a IoV as follows. The DDPG is a model-independent algorithm, and adopts the advantages of a value-based approach and a policy gradient approach. It uses two neural network structures: the Actor network, which is responsible for generating actions based on the current state of the environment, and the Critic network, which evaluates the expected returns when executing above actions. In the process of task offloading, based on its current state and environment information, the DDPG allows each agent to decide whether its task data is performed by using local offloading model or RSU offloading model. In addition, the feedback of states and actions generated by the Actor network are stored in the playback memory (i.e., the replay memory), and then the small batch data is sampled to train the network and update the evaluation functions and strategies. The whole framework of DDPG is shown in Fig.2.

MADDPG framework: Fig. 3 shows the framework of MADDPG algorithm. On the basis of DDPG, the MADDPG is introduced to solve the challenges encountered by multiple agents in IoV. MADDPG adapts the single-agent framework of DDPG to accommodate the dynamics and uncertainty prevalent in multi-agent environments. Each agent of the MADDPG has its own Actor network and Critic network, different from the DDPG, they need to be trained by considering potential strategies of other agents. In this way, each agent updates its network not only based on the individual rewards, but also based on the overall system performance, facilitating collaboration between all agents and the achievement of their common goals. This is particularly important in the application of the IoV, since the information interaction and resource sharing among vehicles are critical to achieving the optimal decision of task offloading. In MADDPG, the Actor network of agents is responsible for making decision actions based on its partial observations, while the Critic network evaluates the value of these actions when considering global observations of the actions of other agents. Finally, MADDPG integrates the local observations and actions of all agents into a global

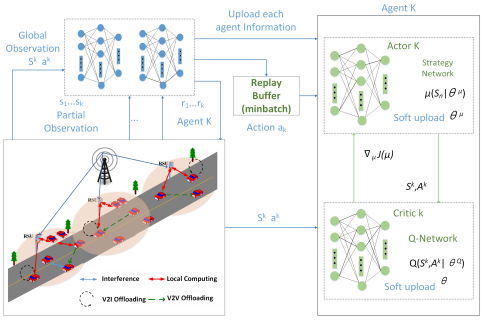

Fig. 3. The framework of MADDPG.

observation, and then the collaboration among the agents and the realization of their common goals are achieved.

To sum up, the pseudo-codes of MADDPG are given in Algorithm 1. Finally, corresponding time complexities and convergences are analyzed.

C. Time Complexity of Analyses of DDPG and MADDPG

The time complexity of MADDPG algorithm mainly depends on the number of system parameters, complexity of environment interactions, and number of training iterations. In the context of multiple agents, each agent has its own policy network and value function network, its time complexity is $O(TK(G1+G2+G3))$, where K is the number of agents/vehicles, $G1$ and $G2$ represent the number of parameters in each agent's policy network and value function network respectively, $G3$ denotes the complexity of environment interactions, and T is the number of iterations in the training process, which demonstrates that the time complexity increases linearly with the number of agents.

D. Convergence Analyses of MADDPG

The convergence of MADDPG algorithm depend on the formula description of the Actor updating and the Critic updating. For DDPG, the policy updating follows a gradient direction, namely $\overline{\nabla}_{\theta_{ve}^{\mu}} J(\theta_{ve}^{\mu})$, to maximize the state-action value function $Q_{ve}(\mathbf{S}(t), \mathbf{A}(t))$, and the state-action value function can be updated by minimizing the loss function of the target network $L(\theta_{ve}^{Q})$, namely Eq. (15). For the MADDPG, it extends above process to a scenario of multiple agents, where the policy updating of each agent aims at maximizing the expected cumulative returns based on its policy gradient and these of other agents. By updating continuously the parameters of the policy and value function, MADDPG converges to the optimum or approximate optimum, which depends on the learning rate, reward design and environmental dynamics.

Algorithm 1 Multi-Agent Deep Deterministic Policy Gradient (MADDPG)

Input: State space $\mathbf{S_1}, ..., \mathbf{S_K}$,, action space $\mathbf{A_1}, ..., \mathbf{A_K}$, for N agents

Initialize: For each agent $i = 1, ..., N$:
-Weight of the Actor network $\mu_{ve}(s|\theta_{ve}^{\mu})$ and Critic network $Q_i(s, a_i, ..., a_K|\theta_{ve}^{Q})$
-Target Actor Network $\mu'_{ve}(s|\theta^{\mu'_{ve}})$ and Target Critic network $Q'_{ve}(s, a_1, ..., a_K|\theta^{Q'_{ve}})$
-Experience playback buffer $\mathbf{D}$
-Noise process $\mathbf{N}$ is used for exploration
-Learning rate λ_{μ}, λ_{Q}, soft update parameter ϖ
for each episode = $1 \rightarrow \mathbf{M}$ **do**
  Initialize the random process N for action exploration
  Receive initial status $s(1)$
  for $t = 1 \rightarrow \mathbf{T}$ **do**
    for each agent i **do**
      Select actions based on the current policy and explore noise: $a(t) = \mu_i(s(t)|\theta_i^{\mu}) + N$
    end for
    Perform action $A(t) = (a_t^1, ..., a_t^K)$, and observe reward $r(s(t), a(t))$ and new state $s(t+1)$
    for each agent i **do**
      Store conversion $(s(t), a(t), r(s(t), a(t)), s(t+1))$ in D_i
    end for
    for each agent i **do**
      Randomly extract a small batch of conversions from D_i
      for each sample **do**
        Set $y_i = r_i + \gamma Q'_i(s_(i+1), \mu'_1(s_(i+1)|\theta_1^{\mu'}), ..., \mu_N\prime(s_(i+1)|\theta_K^{\mu'}|\theta_i^{Q'})$
        Update Critic network to minimize losses: $L_i = \frac{1}{K}\sum(y_i - Q_i(s_i, a_i, ..., a_N|\theta_i^{Q}))^2$
        Update Actor networks using gradient rise: $\nabla\theta_i^{\mu} J_i \approx \frac{1}{K}\sum \nabla a_i Q_i(s, a_1, ..., a_N|\theta^{Q_i})|s = s_i, a_i = \mu_i(s_i)\nabla\theta^{\mu_i}\mu_i(s|\theta^{\mu_i})|s_i$
      end for
      Update target network parameters:
      $\theta^{Q'_i} \leftarrow \varpi\theta^{Q_i} + (1-\varpi)\theta^{Q'_i}$
      $\theta^{\mu'_i} \leftarrow \varpi\theta^{\mu_i} + (1-\varpi)\theta^{\mu'_i}$
    end for
  end for
end for

V. Experimental Simulation

A. Experimental parameter setting

The wireless communication in IoV is simulated according to 3GPP TR 36.885, including the vehicle, lane, and wireless communication network model [35]. The RSU was evenly distributed in a VEC environment with an area of 1km×1km, and the service range of each RSU is a disc centered at the RSU with the radius of 120m. For the vehicles in the system, they move according to the established trajectory. In the process of movement, the vehicle requesting for task offloading can calculate the task data locally, or considering effective within the communication range, unload the task data to parked vehicles, moving vehicles, as well as the RSU. The CPU frequency of the RSU varies between 7GHz and 8GHz, and that of the vehicles changes between 0.1GHz and 0.9GHz. The channel bandwidth of the vehicle and the RSU is 18

TABLE II
SIMULATION PARAMETER SETTINGS

Symbol	Symbolic meaning	Value
K	number of vehicles needing task offloading	16 [23], [31]
F^I	computing resources of vehicles	[0.1, 0.9]GHz [13]
F^R	computing resources of RSUs	[7, 8]GHz [10]
σ^2	noise power	-174 dBm/Hz
d_{ve_k,r_i}	minimum interval among vehicles	10m
v_k	vehicle speed	[30, 150]km/h [31]
R	Number of RSUs	5
Z	task data size	[5, 10, 15]MB [31]
W	bandwidth	18MHz
M	number of parked vehicles	4
γ	reward return value	0.9
ϖ	update rate	0.01
α	weight factor for the delay	0.5
β	weight factor for the energy consumption	0.5

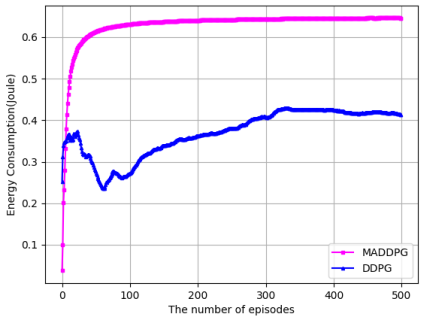

Fig. 5. Energy consumption of MADDPG and DDPG over the number of episodes.

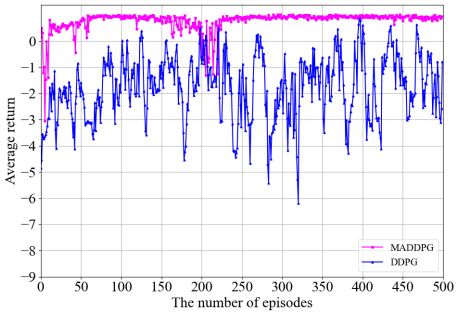

Fig. 4. Average return of MADDPG and DDPG over the number of episodes.

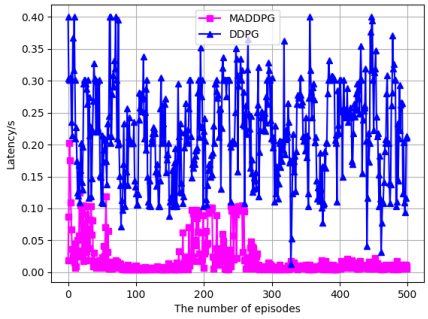

Fig. 6. Latency of MADDPG and DDPG over the number of episodes.

MHz, and the transmission power of the vehicles varies from the range of $[400, 600]$mW. The maximum affordable tolerated delay of the task offloading for all vehicles changes between 100ms and 500ms.

B. Experimental Results of DDPG and MADDPG

Fig. 4 demonstrates the relationship between the average return and the number of training episodes. With the increment of the number of training episodes, the differences of the MADDPG's average return becomes not significant, while that of DDPG exhibits significant fluctuations in average return. On average, the average return of the MADDPG algorithm has increased by approximately 67% compared to that of the DDPG algorithm. This substantial performance enhancement suggests that the MADDPG algorithm possesses superior strategy optimization capabilities in managing tasks within multi-agent environments, making it particularly suitable for IoV systems that demand high stability and efficiency.

The energy consumption under different settings of training episodes are shown in Fig. 5. As the number of training episodes increases, both MADDPG and DDPG algorithms experience an initial rise in energy consumption before stabilizing. Moreover, energy consumption of MADDPG quickly ascends to a stable value of 0.66, while DDPG's consumption levels is relatively at a lower value of 0.43. This indicates that after sufficient training cycles, MADDPG consumes about 50% more energy than DDPG [23]. The higher energy requirement of MADDPG is attributed to its greater computational demands when searching for optimized strategies within multi-agent environments. Moreover, MADDPG's collaborative optimization mechanism enables the execution of more complex task offloading decisions in multi-agent settings, which may lead to reduced overall energy consumption and enhanced system performance in the long run. Therefore, although its has a higher energy consumption during training, MADDPG remains an effective choice for task offloading, especially in scenarios requiring sophisticated multi-agent coordination.

Fig. 6 demonstrates describes the processing delay within 500 training episodes. as the number of training episodes increases, the latency of MADDPG algorithm stabilizes at a relatively low level, while that of DDPG algorithm exhibits a greater variability and tends to be higher on average. Above phenomenon suggests that MADDPG stabilizes at 0.025s after costing 400 episodes, while that of DDPG varies greatly. On average, the latency of DDPG is about 0.20s. On average, the MADDPG algorithm achieves an approximate improvement of 80% on performance of latency when comparing with DDPG [23].

One possible reason of above significant reduction in latency is that, due to the superior coordination effects of MADDPG in multi-agent systems, it enables more efficient synchronization of decisions and actions in complex environments. It can be concluded that the reinforcement learning algorithm is crucial for reducing system latency, enhancing interactive efficiency, and stabilizing the system, especially in applications like the IoV that demands higher real-time performance.

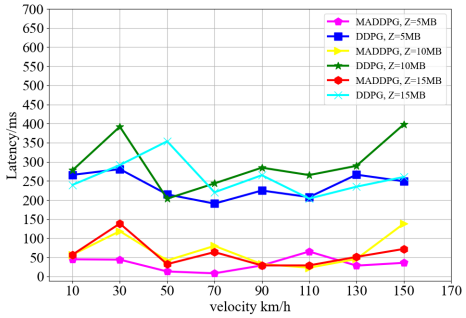

Fig. 7. Energy consumption comparison of MADDPG and DDPG under different settings of vehicular speeds and data sizes.

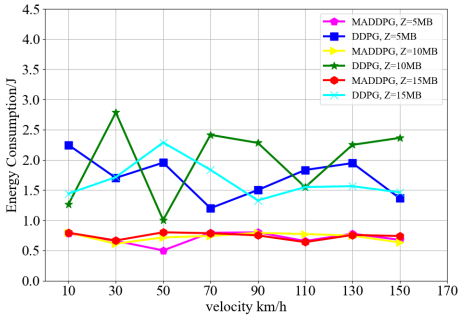

Fig. 9. Energy consumption of MADDPG and DDPG under different settings of vehicular speeds and task sizes.

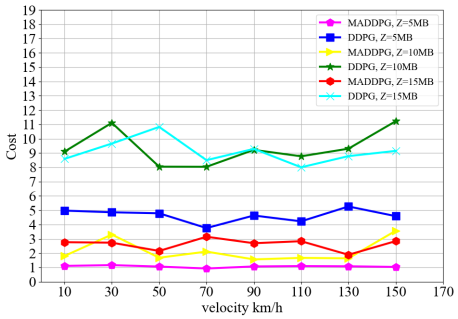

Fig. 8. Cost comparison of MADDPG and DDPG under different settings of vehicle speeds and data sizes.

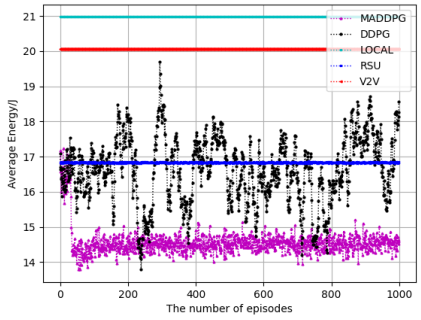

Fig. 10. Average energy consumption comparison under different settings of the number of episodes.

Furthermore, the processing delay of MADDPG and DDPG for different settings of vehicular speeds and task size is shown in Fig. 7. It can be noticed that with a task size of 5MB, the latency of MADDPG improves by approximately 50% compared to DDPG [23]; for a task with size of 15MB, this improvement is about 57%. This indicates that the MADDPG algorithm exhibits superior latency performance when handling larger data loads, particularly in environments with high-velocity vehicles. The enhancement in latency performance of MADDPG attributes to an refined optimization and coordination capability in multi-agent settings. Therefore, MADDPG algorithm may be more advantageous when designing communication and data processing systems for high-speed mobile environments, especially in scenarios with large data volumes and high vehicle speeds.

From Fig. 8, we can see that there is a cost comparison of DDPG and MAPPDG for different settings of vehicular speeds and task size. It can be noticed that a noticeable cost difference exists between the MADDPG and DDPG algorithms at various vehicle speeds (30 km/h, 90 km/h, and 150 km/h) and task sizes (5MB, 10MB, 15MB). For instance, at a speed of 150 km/h and a task size of 15MB, the cost of MADDPG is decreased approximately 42.86% when compared to that of DDPG [23]. This significant cost reduction highlights the efficiency of MADDPG in optimizing expenses, especially at higher speeds and larger data volumes. These observations can provide guidelines for network designers, emphasizing the importance of algorithm selection in scenarios with varying speeds and data demands, demonstrating that under certain conditions, particularly at higher vehicle velocities, MADDPG can offer more cost-effective solutions.

Based on the energy consumption comparison in Fig. 9, we observe the performance of the MADDPG and DDPG algorithms under different vehicle speeds and task sizes settings. Taking 30 km/h, 90 km/h, and 150 km/h as examples, at a data size of 5MB, MADDPG reduces energy consumption by approximately 33.33% compared to DDPG [23]; While for a given task with size of 10MB, the reduction is around 16.67%; And for a given task with size of 15MB, the reduction is about 50%. This suggests that under certain task sizes and vehicular speeds, the MADDPG algorithm is more effective in energy management than the DDPG algorithm, especially when the task demands are larger. These findings can offer practical guidelines for network designers in their selection processes, particularly in the design of IoV systems where energy efficiency is a consideration.

C. Experimental Results of MADDPG and Popular Schemes

To assess the performance of our proposed solutions, we consider the following baselines.

1) LOCAL offloading [8], [9]: The task of each agent was computed only by local server of vehicles;
2) RSU offloading [11], [12]: Each agent can choose to offload the task to the connected RSU;
3) V2V offloading [10], [13]: Each agent chooses to offload the task to the connected parked vehicle and moving vehicle.

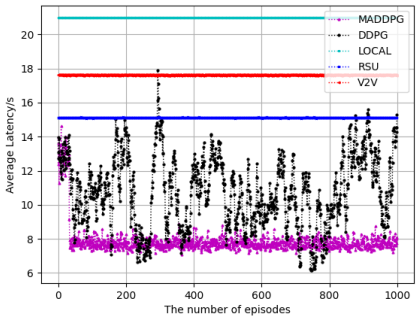

Fig. 11. Average latency comparison under different settings of the number of episodes.

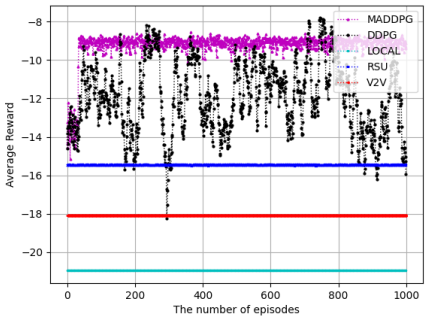

Fig. 12. Average reward comparison under different settings of the number of episodes.

Fig. 10 describes the average energy consumption of all algorithms under different settings of training episodes. On the one hand, it can be observed that the MADDPG algorithm showed a lower energy consumption than other unloading strategies after 1000 training episodes. In contrast, the traditional LOCAL offloading [8], [9], RSU offloading [11], [12], and V2V offloading [10], [13] show a more higher level of energy consumption. Specifically, the energy consumption of the LOCAL unloading strategy changes greatly, which may be due to the uncertainty of the processor load when processing the task data locally. The RSU offloading strategy utilizes the computing power of a fixed infrastructure, but also consumes more energy in dense vehicle areas, because of communication interference and network congestion. The V2V offloading strategy is lower than these of RSU and LOCAL, but compared with MADDPG, they lack a certain adaptability and optimization mechanism, so they are more likely to fail when maintaining the optimal energy consumption state in long-term operation. On the other hand, the MADDPG can better adapt to environmental changes and optimize its offloading decision by using a continuous learning and strategy optimization, which is particularly critical in multi-agent systems, and can effectively reduce the additional energy consumption. To sum up, the MADDPG has obvious advantages in optimizing the energy consumption of task offloading in complex IoV environments, which is particularly important for energy-limited Internet of Vehicles systems.

Fig. 11 provides a comparison of the average delay for different task offloading strategies over 1000 training episodes. Among them, the MADDPG performs well with a stable and low latency performance, which indicates that MADDPG can effectively reduce communication latency during task offloading, and can maintain stability and reliability in a complex multi-agents environment. While the DDPG is slightly worse than MADDPG, but still shows a better performance compared to the schemes of LOCAL offloading [8], [9], RSU offloading [11], [12], and V2V offloading [10], [13]. Specifically, The delay achieved by LOCAL offloading is the highest, due to is limited computing resources. The delay achieved by RSU offloading is higher than these of V2V and MADDPG, which indicates that the communication distance and interference are encountered during task offloading by using computing resource of RSU. The V2V offloading obtains a low latency performance when compared with MADDPG, one possible reason is that there exists a shorter communication distance and less interference. Overall, the high and low latency of the MADDPG strategy in long-term operations demonstrates its advantages in handling task offloading in IoV systems, especially for applications and services that require high real-time performance. Therefore, this study highlights the effectiveness of MADDPG in reducing task unloading delays in complex connected vehicle environments, providing important support for real-time applications in intelligent transportation systems.

In Fig. 12, the performance of average rewards for various task offloading strategies is compared over 1000 training episodes. The MADDPG shows the best performance. The DDPG gives a better relatively performance on processing delay and energy consumption, it cannot obtain a better average reward when compared with MADDPG. The LOCAL exhibits the lowest average rewards, and the RSU offloading strategy achieves a better relatively average reward than LOCAL, but it still presents a relatively worse performance for a higher traffic density. As described by the black line, the average return of DDPG fluctuates markedly [23]. On average, its the average return still is higher than these of V2V offloading strategy and RSU offloading strategy, but behaves worse when compared with that of MADDPG.

In summary, the MADDPG strategy not only shows a lower processing latency but also presents a higher stability in task offloading of IoV, which further demonstrates the effectiveness of our analyses. In addition, these findings provide significant insights for enhancing the system performance and offer practical guidelines for ensuring real-time and reliable applications and resource loading balance of the IoV system.

VI. Conclusion

In this paper, we investigated the task offloading technology in the Internet of Vehicle (IoV), by integrating computing resources of requested vehicles, parked vehicles, moving vehicles and RSUs, with the purpose of minimizing the processing latency and energy consumption of computational tasks. The task offloading of vehicles and the allocation of computational resources in IoV were modeled as a MDP, and the MADDPG algorithm was employed to solve the problem. Furthermore,

the time complexity and convergence of MADDPG were analyzed. Finally, simulations validate the impact of the number of episodes, vehicle speed on the energy consumption, processing delay, convergence and system cost. In particular, compared with the current popular offloading technologies, the MAPPDG shows the best performance on average. It can be noticed that the performance of task offloading depends on the vehicular mobility. Therefore, in our future work, we will devote into vehicle trajectory prediction to enhance the success probability of task offloading. In addition, the integration of unmanned aerial vehicles (UAV) into the IoV can further enhance the network coverage and adjust computational resource allocation more flexibly, which deserves further investigation.

REFERENCES

[1] J. Huang, J. Wan, B. Lv, Q. Ye, and Y. Chen, "Joint computation offloading and resource allocation for edge-cloud collaboration in internet of vehicles via deep reinforcement learning," *IEEE Systems Journal*, vol. 17, no. 2, pp. 2500–2511, 2023.

[2] Z. Ning, K. Zhang, X. Wang, L. Guo, X. Hu, J. Huang, B. Hu, and R. Y. Kwok, "Intelligent edge computing in internet of vehicles: A joint computation offloading and caching solution," *IEEE Transactions on Intelligent Transportation Systems*, vol. 22, no. 4, pp. 2212–2225, 2020.

[3] F. Jiang, W. Liu, J. Wang, and X. Liu, "Q-learning based task offloading and resource allocation scheme for internet of vehicles," in *2020 IEEE/CIC International Conference on Communications in China (ICCC)*. IEEE, 2020, pp. 460–465.

[4] H. Zhou, K. Jiang, S. He, G. Min, and J. Wu, "Distributed deep multi-agent reinforcement learning for cooperative edge caching in internet-of-vehicles," *IEEE Transactions on Wireless Communications*, vol. 22, no. 12, pp. 9595–9609, 2023.

[5] D. Zhang, W. Wang, J. Zhang, T. Zhang, J. Du, and C. Yang, "Novel edge caching approach based on multi-agent deep reinforcement learning for internet of vehicles," *IEEE Transactions on Intelligent Transportation Systems*, vol. 24, no. 8, pp. 8324–8338, 2023.

[6] H. Gao, X. Wang, W. Wei, A. Al-Dulaimi, and Y. Xu, "Com-ddpg: Task offloading based on multiagent reinforcement learning for information-communication-enhanced mobile edge computing in the internet of vehicles," *IEEE Transactions on Vehicular Technology*, vol. 73, no. 1, pp. 348–361, 2024.

[7] W. Fan, Y. Su, J. Liu, S. Li, W. Huang, F. Wu, and Y. Liu, "Joint task offloading and resource allocation for vehicular edge computing based on v2i and v2v modes," *IEEE Transactions on Intelligent Transportation Systems*, vol. 24, no. 4, pp. 4277–4292, 2023.

[8] A. Naouri, H. Wu, N. A. Nouri, S. Dhelim, and H. Ning, "A novel framework for mobile-edge computing by optimizing task offloading," *IEEE Internet of Things Journal*, vol. 8, no. 16, pp. 13 065–13 076, 2021.

[9] B. Kar, W. Yahya, Y.-D. Lin, and A. Ali, "Offloading using traditional optimization and machine learning in federated cloud–edge–fog systems: A survey," *IEEE Communications Surveys & Tutorials*, vol. 25, no. 2, pp. 1199–1226, 2023.

[10] J. Shi, J. Du, Y. Shen, J. Wang, J. Yuan, and Z. Han, "Drl-based v2v computation offloading for blockchain-enabled vehicular networks," *IEEE Transactions on Mobile Computing*, vol. 22, no. 7, pp. 3882–3897, 2023.

[11] G. Raja, A. Ganapathisubramaniyan, S. Anbalagan, S. B. M. Baskaran, K. Raja, and A. K. Bashir, "Intelligent reward-based data offloading in next-generation vehicular networks," *IEEE Internet of Things Journal*, vol. 7, no. 5, pp. 3747–3758, 2020.

[12] Y. Wu, L. P. Qian, H. Mao, X. Yang, H. Zhou, X. Tan, and D. H. Tsang, "Secrecy-driven resource management for vehicular computation offloading networks," *IEEE Network*, vol. 32, no. 3, pp. 84–91, 2018.

[13] F. Liu, J. Chen, Q. Zhang, and B. Li, "Online mec offloading for v2v networks," *IEEE Transactions on Mobile Computing*, vol. 22, no. 10, pp. 6097–6109, 2023.

[14] C. Chen, L. Chen, L. Liu, S. He, X. Yuan, D. Lan, and Z. Chen, "Delay-optimized v2v-based computation offloading in urban vehicular edge computing and networks," *IEEE Access*, vol. 8, pp. 18 863–18 873, 2020.

[15] X. Xu, X. Zhang, X. Liu, J. Jiang, L. Qi, and M. Z. A. Bhuiyan, "Adaptive computation offloading with edge for 5g-envisioned internet of connected vehicles," *IEEE Transactions on Intelligent Transportation Systems*, vol. 22, no. 8, pp. 5213–5222, 2020.

[16] M. Zhu, Y. Hou, X. Tao, T. Sui, and L. Gao, "Joint optimal allocation of wireless resource and mec computation capability in vehicular network," in *2020 IEEE Wireless Communications and Networking Conference Workshops (WCNCW)*. IEEE, 2020, pp. 1–6.

[17] Z. Zhou, J. Feng, Z. Chang, and X. Shen, "Energy-efficient edge computing service provisioning for vehicular networks: A consensus admm approach," *IEEE Transactions on Vehicular Technology*, vol. 68, no. 5, pp. 5087–5099, 2019.

[18] X. Wang, Z. Ning, S. Guo, and L. Wang, "Imitation learning enabled task scheduling for online vehicular edge computing," *IEEE Transactions on Mobile Computing*, vol. 21, no. 2, pp. 598–611, 2020.

[19] W. Feng, N. Zhang, S. Li, S. Lin, R. Ning, S. Yang, and Y. Gao, "Latency minimization of reverse offloading in vehicular edge computing," *IEEE Transactions on Vehicular Technology*, vol. 71, no. 5, pp. 5343–5357, 2022.

[20] X. Xu, Y. Xue, X. Li, L. Qi, and S. Wan, "A computation offloading method for edge computing with vehicle-to-everything," *IEEE access*, vol. 7, pp. 131 068–131 077, 2019.

[21] X. Dai, Z. Xiao, H. Jiang, H. Chen, G. Min, S. Dustdar, and J. Cao, "A learning-based approach for vehicle-to-vehicle computation offloading," *IEEE Internet of Things Journal*, vol. 10, no. 8, pp. 7244–7258, 2022.

[22] X. Hou, Z. Ren, J. Wang, W. Cheng, Y. Ren, K.-C. Chen, and H. Zhang, "Reliable computation offloading for edge-computing-enabled software-defined iov," *IEEE Internet of Things Journal*, vol. 7, no. 8, pp. 7097–7111, 2020.

[23] X. Huang, L. He, X. Chen, L. Wang, and F. Li, "Revenue and energy efficiency-driven delay-constrained computing task offloading and resource allocation in a vehicular edge computing network: A deep reinforcement learning approach," *IEEE Internet of Things Journal*, vol. 9, no. 11, pp. 8852–8868, 2021.

[24] C.-M. Huang, S.-Y. Lin, and Z.-Y. Wu, "The k-hop-limited v2v2i vanet data offloading using the mobile edge computing (mec) mechanism," *Vehicular Communications*, vol. 26, no. 8, p. 100268, 2020.

[25] S. Raza, S. Wang, M. Ahmed, M. R. Anwar, M. A. Mirza, and W. U. Khan, "Task offloading and resource allocation for iov using 5g nr-v2x communication," *IEEE Internet of Things Journal*, vol. 9, no. 13, pp. 10 397–10 410, 2021.

[26] B. Hazarika, K. Singh, S. Biswas, and C.-P. Li, "Drl-based resource allocation for computation offloading in iov networks," *IEEE Transactions on Industrial Informatics*, vol. 18, no. 11, pp. 8027–8038, 2022.

[27] K. Yu, J. Yu, Z. Feng, and H. Chen, "A reassessment on applying protocol interference model under rayleigh fading: From perspective of link scheduling," *IEEE/ACM Transactions on Networking*, vol. 32, no. 1, pp. 238–252, 2024.

[28] K. Yu, J. Yu, X. Cheng, D. Yu, and A. Dong, "Efficient link scheduling solutions for the internet of things under rayleigh fading," *IEEE/ACM Transactions on Networking*, vol. 29, no. 6, pp. 2508–2521, 2021.

[29] J. Zhao, Q. Li, Y. Gong, and K. Zhang, "Computation offloading and resource allocation for cloud assisted mobile edge computing in vehicular networks," *IEEE Transactions on Vehicular Technology*, vol. 68, no. 8, pp. 7944–7956, 2019.

[30] X. Zhang, W. Wu, Z. Zhao, J. Wang, and S. Liu, "Rmddqn-learning: Computation offloading algorithm based on dynamic adaptive multi - objective reinforcement learning in internet of vehicles," *IEEE Transactions on Vehicular Technology*, vol. 72, no. 9, pp. 11 374–11 388, 2023.

[31] L. Zhu, Z. Zhang, P. Lin, O. Shafiq, Y. Zhang, and F. R. Yu, "Learning-based load-aware heterogeneous vehicular edge computing," in *GLOBECOM 2022 - 2022 IEEE Global Communications Conference*, 2022, pp. 4583–4588.

[32] R. Lowe, Y. I. Wu, A. Tamar, J. Harb, O. Pieter Abbeel, and I. Mordatch, "Multi-agent actor-critic for mixed cooperative-competitive environments," *Advances in neural information processing systems*, vol. 30, 2017.

[33] W. Duan, X. Li, Y. Huang, H. Cao, and X. Zhang, "Multi-agent-deep-reinforcement-learning-enabled offloading scheme for energy minimization in vehicle-to-everything communication systems," *Electronics*, vol. 13, no. 3, p. 663, 2024.

[34] Y. Sun, X. Guo, J. Song, S. Zhou, Z. Jiang, X. Liu, and Z. Niu, "Adaptive learning-based task offloading for vehicular edge computing systems," *IEEE Transactions on vehicular technology*, vol. 68, no. 4, pp. 3061–3074, 2019.

[35] H. Yang, X. Xie, and M. Kadoch, "Intelligent resource management based on reinforcement learning for ultra-reliable and low-latency iov communication networks," *IEEE Transactions on Vehicular Technology*, vol. 68, no. 5, pp. 4157–4169, 2019.